Polymer surface and thin film vibrational dynamics of poly(methyl methacrylate), polybutadiene, and polystyrene

Miriam A. Freedman,[a] James S. Becker, A. W. Rosenbaum,[b] and S. J. Sibener[c]
The James Franck Institute and Department of Chemistry, The University of Chicago, 929 E. 57th St., Chicago, Illinois 60637, USA

(Received 7 February 2008; accepted 12 May 2008; published online 28 July 2008)

Inelastic helium atom scattering has been used to investigate the vibrational dynamics at the polymer vacuum interface of poly(methyl methacrylate), polystyrene, and polybutadiene thin films on SiO_x/Si(100). Experiments were performed for a large range of surface temperatures below and above the glass transition of these three polymers. The broad multiphonon feature that arises in the inelastic scattering spectra at surface temperatures between 175 and 500 K is indicative of the excitation of a continuum of surface vibrational modes. Similarities exist in the line shapes of the scattering spectra, indicating that helium atoms scatter from groups of similar mass on the surface of these polymer thin films. The line shapes obtained were further analyzed using a semiclassical scattering model. This study has shown that quite different polymer thin films can have similar interfacial dynamics at the topmost molecular layer. © *2008 American Institute of Physics*. [DOI: 10.1063/1.2939018]

I. INTRODUCTION

Polymer thin films are widely used in the fabrication of devices for technological applications such as microelectronics, sensors, protective and optical coatings, and membranes for diverse fields from engineering and material science to medicine.[1] Significant questions remain, however, regarding the differences between the structure and properties of these films as compared to bulk polymer samples.[2] In particular, nanoconfinement strongly affects the overall film properties due to the increased free volume and difference in electrostatic potential at the free surface and interactions with the substrate layer. Investigation into these differences began over a decade ago with the dewetting studies of Reiter and the ellipsometry studies of Keddie *et al.*[3] Many aspects of polymer thin films have been studied using a variety of techniques. For studies of the glass transition averaged over the whole thin film system, areas of interest include (but are not limited to) the effect of the substrate layer,[4] the importance of the molecular architecture and tacticity of the polymer,[5] molecular weight,[6] relaxation,[7] and diffusion of small particles through the film.[8] Numerous studies have also been performed to investigate increased mobility in the surface layer. Areas of interest include α-relaxation,[9] surface molecular motion as probed by scanning probe microscopy,[10] surface relaxation studied with sum frequency generation (SFG),[11] and relaxation after surface deformation.[12] The majority of dynamics studies that have been performed probe long length-scale motion of polymer chains or segmental motion. One exception is neutron scattering studies in which molecular-scale motion of the polymers is observed. Most of the techniques used either perturb the system of interest or probe several layers rather than just the topmost interface, and so questions regarding the properties of the interface at the free surface of the polymer remain largely unanswered.

To characterize the dynamics at the topmost interface, we use the nondestructive and surface-sensitive probe of low-energy helium atom scattering (HAS). With the exception of our previous study,[13] this technique has not been used to investigate polymer thin films. This study is both different from traditional HAS and from most studies of polymer thin film dynamics. As a result, a description of what we can uniquely measure with HAS is presented. HAS has traditionally been used to investigate the structure and dynamics of single crystals and simple adsorbates on single crystals.[14,15] HAS can be viewed as a surface-sensitive analog to neutron scattering. Because helium atoms scatter from the electron density approximately 3 Å above the surface whereas neutrons scatter from atomic cores, HAS provides increased surface sensitivity.[15–17] HAS has been used to characterize surface structure and is remarkably sensitive to defects including point defects and steps.[18] In dynamics studies, HAS has been used to characterize phonon dispersion curves with inelastic HAS, diffusion through quasielastic HAS, and multiphonon scattering.

In recent years, helium atom scattering studies have expanded to include the investigation of organic thin films. Studies have probed structure, where possible, and dynamics of self-assembled monolayers (SAMs),[19] alkanes,[20] carboxylic acids,[21] liquids,[22] and fatty acids.[23] In most of these cases, the surface is ordered as observed with helium atom diffraction. Single-phonon spectra are often found, sometimes over

[a]Present address: Cooperative Institute for Research in Environmental Sciences, University of Colorado, Boulder, CO 80309.
[b]Present address: Intel Corporation, 2111 NE 25th Ave., Hillsboro, OR 97124.
[c]Author to whom correspondence should be addressed. Electronic mail: s-sibener@uchicago.edu.

TABLE I. Parameters used for polymer experiments. M_w is the molecular weight, M_w/M_n is the polydispersity index, T_g is the glass transition temperature, h is the film thickness, and R_g is the radius of gyration. Thicknesses are given both in units of nanometers and radius of gyration.

Polymer	M_w (kg/mol)	M_w/M_n	T_g (K)	h (nm)	R_g (nm)[a]	h (R_g)
Poly(methyl methacrylate)	350	1.15	380	11	15	0.67
Poly(methyl methacrylate)	350	1.15	380	47	15	3.3
1,4-trans-Polybutadiene	60.9	1.05	167	16	7.1	2.2
1,4-trans-Polybutadiene	60.9	1.05	167	87	7.1	12
Polystyrene	400	1.06	373	119	17	7.0
Polystyrene	400	1.06	373	111	17	6.5

[a]Values for R_g for PB from Ref. 25.

a broad multiphonon background. In some cases, however, only a multiphonon feature is observed,[22,23] as is the case with polymer thin films. With the precedent of HAS studies on organic mono- and multilayers, in our group, we have decided to investigate polymer thin films. Helium atom scattering provides a detailed picture of the low-energy surface vibrational dynamics of the polymer at the vacuum interface. The information we obtain is in some ways more similar to heavy rare gas scattering studies of complex materials,[22,24] rather than traditional HAS experiments. The use of helium atoms, however, provides a nondestructive and surface-sensitive probe through which we can characterize vibrational dynamics of the topmost interfacial layer.

Additionally, HAS studies of polymer thin films are more similar to previous neutron scattering studies than to other techniques commonly used in the polymer literature. In particular, HAS is sensitive to molecular-scale vibrational dynamics rather than segmental or long-range motion of the polymer chains. In contrast to neutron scattering studies, HAS is sensitive exclusively to the topmost molecular layer. The vibrations probed are sagittally polarized modes of the chain or substituent groups present at the polymer-vacuum interface. Localized, short timescale motion of the topmost molecular interface in confined polymer systems has not been investigated in the literature. Information about surface vibrational motion would provide new information that would help to develop a better understanding of dynamics in confined polymer systems.

Helium atom scattering is uniquely able to access information on the dynamics and corrugation of the polymer-vacuum interface without complicating contributions from the bulk properties. In a previous paper, we have shown helium atom scattering to be sensitive to the effect of nanoconfinement on the vibrational dynamics of poly(methyl methacrylate) (PMMA) in the thin film limit.[13] In this paper, we significantly expand on our prior work by examining and comparing more extensive results for PMMA, which has a bulk glass transition temperature of 380 K, to 1,4-*trans*-polybutadiene (PB), which has a bulk glass transition temperature of 167 K, over the temperature range of 200–500 K.[25] We also compare our PMMA results to those from polystyrene (PS) (bulk T_g=373 K), one of the most widely studied polymers. Moreover, in this work, we also present a detailed analysis of the scattering spectra for all three systems, utilizing a semiclassical scattering model from which we derive information about the He-polymer potential energy surface, polymer surface structure, and the surface's molecular-scale vibrational dynamics.

II. EXPERIMENTAL

Experiments were conducted in a high angle- and energy-resolution helium atom scattering apparatus, which has been described in detail elsewhere.[26] Briefly, it consists of a cryogenically cooled supersonic helium beam source, an ultrahigh vacuum (UHV) scattering chamber equipped with surface characterization tools, a precollision chopper (chopper to sample distance of 0.554 m), and a rotating, long flight path (sample to ionizer distance of 1.005 m) quadrupole mass spectrometer detector. The rotating detector and independent crystal angular drive allow for the incident and final angles to be independently varied. The angular collimation yields a resolution of 0.22° and a $\Delta\nu/\nu$ of less than 1% for most of the reported beam energies. This design allows for precise measurements of scattering angles and energy exchange with the surface by acquisition of the time-of-flight (TOF) of scattered helium atoms. A cross-correlation TOF technique with a pseudorandom chopping sequence was used to maximize the signal-to-noise ratio.[27] Spectra are deconvoluted according to Ref. 28.

Three high-molecular weight, atactic polymers, PMMA (PolySciences), 1,4-*trans*-PB (Polymer Source), and PS (PolySciences), were spin coated on the native oxide layer of Si(100). Parameters for the molecular weight, polydispersity, and thickness of the samples can be found in Table I. Please note that we have provided the relative thicknesses in terms of the bulk radius of gyration, R_g. This scaling is common and is generally useful for comparing polymers of different molecular weights. The scaling cannot, however, be exactly correlated with actual film thickness because the chain conformation of polymers, and hence their radius of gyration, changes in a thin film relative to the bulk. The SiO_x/Si(100) substrates were cleaned by sequential sonication in toluene, acetone, and methanol. The substrates used for the PB films were additionally cleaned by 10 min immersions in 80 °C solutions of 5:1:1 H_2O:30% H_2O_2:NH_4OH followed by 6:1:1 H_2O:30% H_2O_2:40% HCl. The substrates were then

treated for 6.5 min in 40% NH_4F in MeOH to create flat hydrophobic terraces.[29] The hydrogen-terminated substrate degrades quickly, so the PB samples were spun immediately following treatment and drying. In addition, the 119 nm thick sample of PS was made using this sample preparation. The thin films were annealed under argon for 120 min at 413 K for PMMA and 443 K for PS. PB was not annealed prior to insertion in the UHV chamber because it was prepared at a temperature far above its glass transition. The sample thickness was measured *ex situ* by ellipsometry. Optical microscopy and atomic force microscopy were used to further assess the smoothness of the film. PMMA and PS samples were inserted in the scattering chamber (base pressure of 10^{-9}–10^{-10} torr) and annealed at the beginning of each experimental run at 440 K for 30 min. PB samples were annealed at 300 K overnight. The samples were subsequently cooled at 5 K/min to the lowest temperature used and spectra were taken for the various temperatures. Changes to the cooling rate from 2 K/min to approximately 35 K/min did not have any affect on the results. Because of the low scattering signal from the polymers, highly ordered pyrolitic graphite was used for calibration of the beam. From thermogravimetric analysis, the PMMA sample began to degrade at temperatures above approximately 550 K in a nitrogen atmosphere, which agrees well with the literature value of 543 K.[30] According to the literature, PB compounds containing both *cis* and *trans* components begin to degrade at around 623 K.[31] Bulk PS begins to degrade above 548 K.[25] Scattering experiments were therefore not performed at temperatures above 490 K for PMMA and 500 K for PS and PB.

III. RESULTS

For PMMA, we obtained spectra for a wide range of parameters at both specular and nonspecular final angles. In the specular geometry, runs were taken at angles of 24.42°, 32.42°, and 37.42° measured with respect to the surface normal for beam energies from 9.7 to 54 meV (4.31 $Å^{-1}$ with ΔK=1.76–10.15 $Å^{-1}$ with ΔK=4.16 $Å^{-1}$) and sample temperatures from 60 to 490 K. Elastic scattering was observed for PMMA at the lowest sample temperatures and beam energies.[13] No elastic scattering was observed at cryogenic surface temperatures and low beam energies for PB. To compare the multiphonon scattering results for PMMA at the higher beam energies, PB and PS spectra were taken at beam energies from 25 to 43 meV. The same scattering geometries were used for PB and PMMA, while scattering from PS was performed in the specular geometry at angles of 25.92°, 30.92°, and 35.92°. No difference was observed between the scattering spectra of PS on hydrophilic and hydrophobic substrates, so these are grouped together for the purpose of this analysis. Raw data from a representative cross-correlation spectrum and the corresponding deconvoluted TOF spectrum are shown in Fig. 1. The intensity, which is transformed into the energy transfer domain, is also plotted in this figure versus the difference between the final and initial energies of the helium beam ΔE.

Figures 2 and 3 show representative spectra for PMMA, PS, and PB under similar scattering geometries, sample temperatures, and beam energies plotted in the time and energy transfer domains, respectively. As the sample temperature is increased, the intensity of the maximum decreases. In Fig. 2, it is shown that as the surface temperature increases, the maximum intensity moves to earlier times. In Fig. 3, this shift corresponds to a slight change in the position of the intensity maximum to higher ΔE. The high energy tail also grows, as expected due to an increase in annihilation contributions to the collisional energy transfer. The intensity maximum occurs in the energy-loss region, i.e., at negative ΔE. In both figures, the general features are the same for each polymer, with broad asymmetric curves that have an intensity maximum at negative ΔE. These trends are observed regardless of sample thickness, beam energy, and scattering geometry. Broad, multiphonon spectra have been observed previously for soft, organic substrates like fatty acid monolayers and SAMs using helium atom scattering.[23,32] From experi-

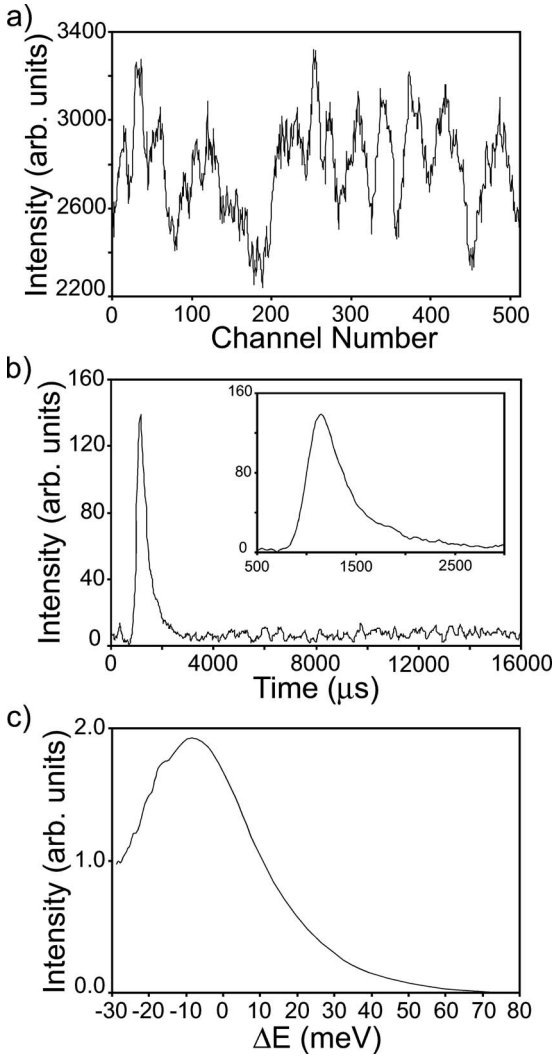

FIG. 1. (a) Representative raw cross-correlation data and (b) the deconvoluted time-of-flight (TOF) spectrum. Signal was obtained for 511 channels using a pseudorandom chopping sequence. Each channel is 32 μs wide, yielding a TOF window from 0 to approximately 16 ms. The inset in (b) shows the line shape of the feature over a smaller time domain. The data were obtained from scattering from polystyrene with a surface temperature of 200 K, a beam energy of 43 meV, and initial and final angles of 25.92°. (c) The same spectrum shown in the energy transfer domain.

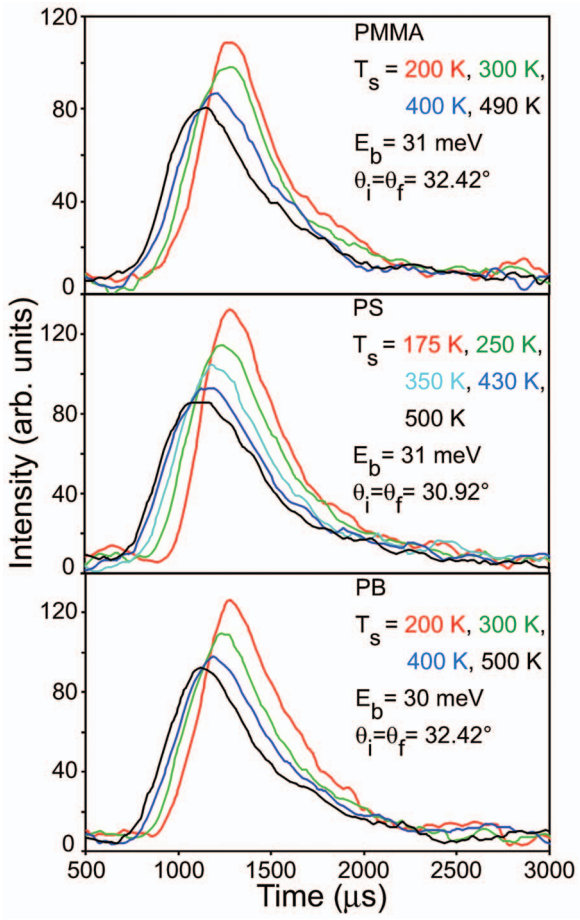

FIG. 2. (Color) Inelastic scattering spectra for PMMA, PS, and PB. Multiple spectra are included for each polymer, covering a wide range of surface temperatures. The intensity of the peak maximum decreases with increasing surface temperature while the intensity of the tail increases.

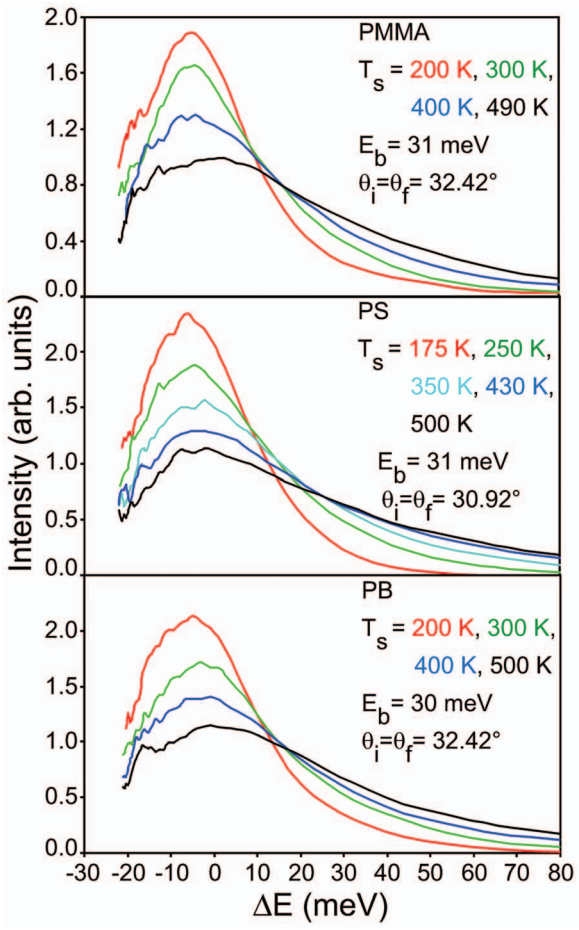

FIG. 3. (Color) The same as Fig. 2, but in the energy transfer domain. ΔE is the difference between the final and initial energies of the helium beam.

ments performed to determine the angular position of maximum scattered intensity using PMMA with an incident angle of 32.42° and a surface temperature of 200 K, we find that maximum scattered intensity occurs at a final angle more than 8° closer to the surface normal. The intensity is a slowly varying function of angle. At higher temperatures, the position of maximum intensity shifts farther toward the surface normal.

Spectra from the three different polymers taken at similar beam energies, sample temperatures, and scattering geometries have been overlaid at each surface temperature (Fig. 4). The spectra are scaled by the maximum intensity at an intermediate surface temperature. For example, in Fig. 4, the peak maximum of the data taken at a sample temperature of 350 K is set to unity. No other normalization is done to change the intensity or shape of these curves. Spectra taken at all sample temperatures are then scaled by this maximum intensity. The line shapes of the spectra for the three polymers can then be compared at each temperature. By scaling all the spectra by the 350 K maximum intensity, the rate of intensity decay with surface temperature can also be analyzed. This figure shows that the scattering spectra arising from the three different polymers are virtually superimposable. In particular, the intensity decay and line shape are similar for all polymers. Slight differences in intensities in Fig. 4 are observed due to variations in surface temperature. Specifically, the PS spectrum in the top plot is taken at a sample temperature of 175 K and the PMMA spectrum in the bottom plot is at a sample temperature 490 K. Differences in the width of the spectra of the thinnest PMMA samples have been discussed in a previous paper.[13]

Figures 5 and 6 show a comparison of PB spectra with two different beam energies in the time and energy transfer domains, respectively. In the time domain, the scattering spectra appear similar, but the spectra taken with the higher energy beam are translated to earlier times. In the energy transfer domain, the energy gain, i.e., positive ΔE, tails overlay well, while the positions of the negative ΔE side of the spectra differ considerably. The spectrum arising from a 40.5 meV beam goes to approximately $\Delta E=-30$ meV, whereas the spectrum arising from a 29.7 meV beam goes to approximately $\Delta E=-20$ meV. For the energy-loss ($\Delta E<0$) side of the spectra, a higher beam energy leads to a greater amount of energy transfer to the surface. The similarity between the spectra on the energy gain ($\Delta E>0$) indicates that the probability of annihilating vibrational modes is relatively similar.

IV. REVIEW OF THEORY

The Debye–Waller factor $2w$ determines which features are observed in TOF spectra. For example, for $2w>6$, the

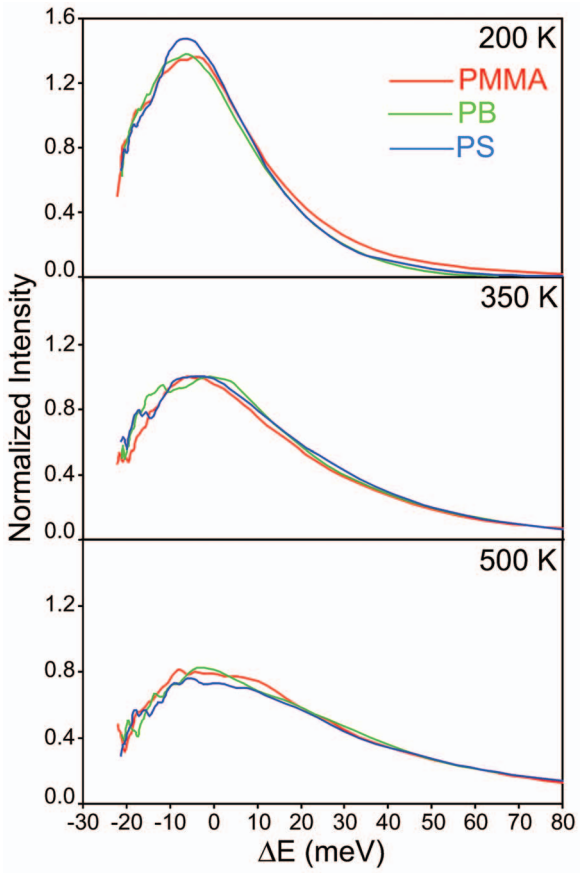

FIG. 4. (Color) The spectra for PMMA (red), PS (blue), and PB (green) are overlaid. The surface temperature is listed in the upper right corner of the spectrum. The maximum intensity at 350 K is set to unity and the other spectra scaled accordingly in order to compare the line shapes and the change in maximum intensity with surface temperature. Other parameters are similar for the polymers with a beam energy of approximately 31 meV and initial and final angles of 24.42° for PMMA and PB and 25.92° for PS. The sample thicknesses are 47 nm for PMMA, 119 nm PS, and 87 nm PB. Differences in the intensities are caused by slight deviations in surface temperature.

multiphonon regime is observed whereas for $2w \ll 1$, only elastic scattering is seen.[33] In the specular geometry, $2w$ is related to the incident beam energy E_i and the surface temperature T_s by[34]

$$2w = \frac{24m(E_i \cos^2 \theta_i + D)T_s}{Mk_B\theta_D^2}, \quad (1)$$

where m is the mass of He, θ_i is the incident angle, D is the Beeby correction,[35] M is the surface mass, and θ_D is the surface Debye temperature. We use a surface Debye temperature of 120 K, as was used for a fatty acid monolayer.[33] We set D to 7 meV, which is close to values for high density alkanethiol SAMs.[36] The well depth may differ slightly for PS compared to PMMA and PB due to the He-phenyl interaction. SFG vibrational spectroscopy studies indicate that the ester methyl groups of PMMA decorate the polymer-air interface, tilted with respect to the surface normal between 0° and 30°, whereas the α-methyl groups lie down on the surface.[37] It is likely, therefore, that helium interacts primarily with the terminal methyl groups on the ester methyl side chain, indicating $M = 15$ amu. SFG vibrational spectroscopy

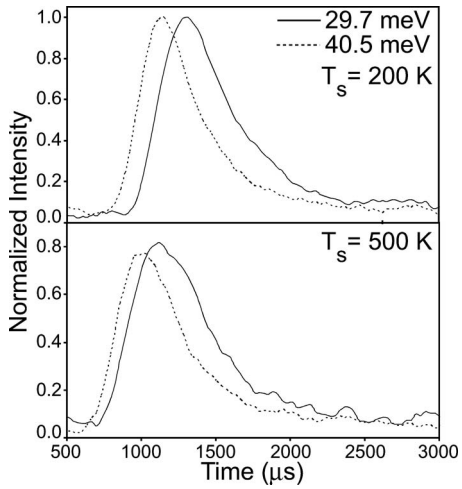

FIG. 5. A comparison of PB spectra with two different beam energies. The polymer film is 87 nm thick with initial and final angles of 24.42° and beam energies of 29.7 meV (—) and 40.5 meV (---). The top spectrum is taken at a sample temperature of 200 K and the bottom spectrum is at 500 K.

of PS indicates that the phenyl groups project normal to the surface, approximately 57° from the surface normal, indicating that collisions occur with CH groups.[38] For PB, the helium atoms should scatter from a mixture of CH and CH_2 groups. Using Eq. (1), we find values of $2w > 15$ for the systems used in this study at beam energies of 30–40 meV. The value of $2w$ increases for angles closer to normal and with increases in surface temperature.

We used a semiclassical model developed by Manson *et al.* to fit the inelastic line shape for the three polymers.[39] Two different models were developed, one in which scattering occurs from a continuum of atomic centers, and one from discrete atomic centers.[40] The former has been used previously for single crystal metal surfaces, and the latter has been used to model scattering from a fatty acid monolayer. In the continuum model, the intensity of the multiphonon spectra decreases with temperature according to $(\hbar\omega_0 k_B T_S)^{-3/2}$, where $\hbar\omega_0$ is the classical recoil velocity. For the discrete model, the temperature dependence is $(\hbar\omega_0 k_B T_S)^{-1/2}$. The classical recoil velocity $\hbar\omega_0$ is given by $\hbar^2 k^2/2M$, where the

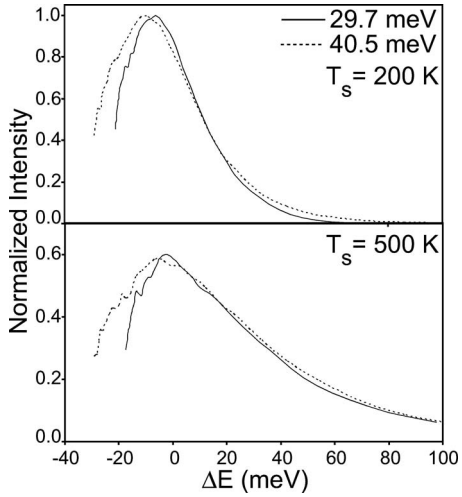

FIG. 6. The same as Fig. 4, but in the energy transfer domain.

total momentum transfer $k=k_f-k_i$ (k_f and k_i are the final and initial momenta, respectively).[33] We have shown previously that the temperature dependence of the discrete model fits the temperature decay of the PMMA data, whereas the continuum model decays too rapidly.[13] Because the rate of decay is similar for the different polymers, the discrete model should be the appropriate one to use for all the spectra presented. The discrete centers model states that the differential reflection coefficient, which gives the number of particles detected per solid angle per unit energy is given by[33]

$$\frac{dR}{d\Omega_f dE_f} \propto |k_f\|\tau_{fi}|^2 \left(\frac{\hbar\pi}{\omega_0 k_B T_s}\right)^{1/2} \exp\left\{-\frac{(\Delta E+\hbar\omega_0)^2}{4k_B T_s \hbar\omega_0}\right\}. \tag{2}$$

The perpendicular components of the momenta are corrected for the He-surface well depth by the Beeby correction. The form factor τ_{fi} is the product of the Jackson–Mott matrix element $v_{\mathrm{JM}}(k_{iz},k_{fz})$ of the potential $v(z)=\exp[-\beta z]$, and a cutoff in parallel momentum.[41] The cutoff factor is given by

$$\tau_{fi} = v_{\mathrm{JM}} \exp\left\{-\frac{\beta^2}{Q_c^2}\left(\left[1+\left(\frac{\Delta K}{\beta}\right)^2\right]^{1/2}-1\right)\right\},$$

where Q_c is the parallel momentum cutoff factor. The Jackson–Mott matrix element is given by

$$v_{\mathrm{JM}}(p,q) = \frac{p-q}{\sinh(p-q)}\frac{p+q}{\sinh(p+q)}\left(\frac{\sinh(2p)\sinh(2q)}{4pq}\right)^{1/2},$$

where p and q are nondimensionalized momenta given by $q=k_{iz}/\beta$ and $p=k_{fz}/\beta$.[41] The parameters β and Q_c are descriptors of the surface structure. Specifically, β is a measure of the relative softness of the surface and Q_c measures the corrugation or roughness of the surface.

V. DISCUSSION

To determine the degree of similarity of the PMMA, PB, and PS spectra beyond the overlay of line shapes shown in Fig. 4, we have plotted the integrated intensity as a function of temperature in Fig. 7. The integrated intensities are calculated from the spectra converted into the energy domain. The absolute intensities are then scaled by the integral of the lowest temperature spectrum in order to be able to compare the spectra. From Fig. 7, it is clear that the intensity decay is virtually identical between the different polymers. Changes to the scattering geometry result in only small changes to the intensity decay. An increase in the beam energy from approximately 30 to approximately 40 meV decreases the rate of the intensity decay by less than a factor of 2.

The un-normalized values for the full width half maximum (FWHM) are shown for each of the polymers at a variety of scattering angles (Fig. 8). At the lower beam energy of 30 meV, the FWHM spans 25–35 meV for the lowest surface temperatures and 43–53 meV for the highest. A close correspondence exists between the different polymers [Fig. 8(a)]. For a beam energy of 40 meV, the FWHM is approximately 30–40 meV at the lowest surface temperatures. At the highest surface temperatures, the FWHM still spans a small range for all polymers of between 50 and 62 meV. No large difference is observed as a function of angle, though the inclusion of this quantity of data does result in some degree of scatter. The higher beam energy should yield larger values for FWHM, as observed, due to the ability of the helium to transfer more energy to the sur-

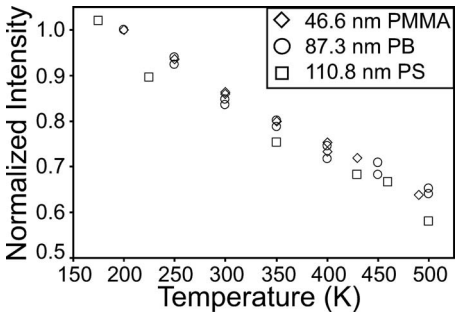

FIG. 7. Decay of the integrated intensity of the inelastic feature calculated from the curves converted to the energy transfer for the polymer thin films. The spectra were taken at a beam energy of 30 meV, with initial and final angles of 24.42° for PMMA and PB, and 25.92° for PS. The intensity at 200 K was normalized for PMMA and PB. The slopes of the intensity decay were then used to determine an average value for these polymers at 175 K, the value of which was used to normalize the PS intensities. The intensity decay rates are -1.2×10^{-3} K^{-1} meV^{-1} for PMMA, -1.1×10^{-3} K^{-1} meV^{-1} for PB, and -1.2×10^{-3} K^{-1} meV^{-1} for PS.

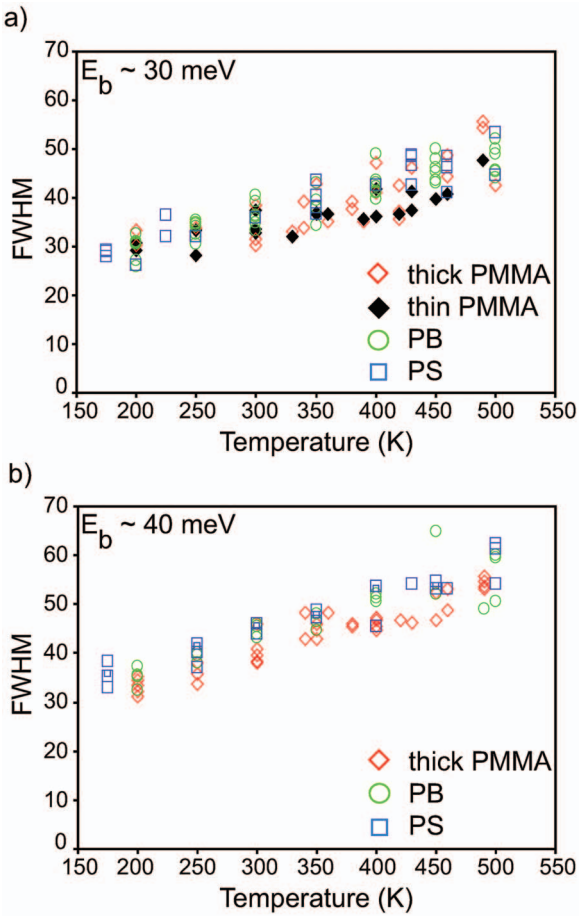

FIG. 8. (Color) The un-normalized full width half maximum of scattering spectra in the energy domain graphed vs surface temperature at two beam energies. Data from scattering in the specular geometry at angles of 24.42°, 32.42°, and 37.42° are shown together.

face. PMMA tends to fall in the lower range of FWHM values, but the FWHM of PS and PB are approximately identical. Figure 8(a) also shows data from the 11 nm PMMA film (labeled "thin" in the figure). We have shown that helium atoms scattering from films of this thickness have a decreased probability of annihilating vibrational modes in the scattering process at more normal angles in comparison with the 47 nm films (labeled "thick" in the figure).[13] The thinner PMMA films do on average have the lowest FWHM, as expected.

From our studies of different thicknesses of PMMA, we have shown that the scattering spectra are highly sensitive to the thickness of the samples.[13] Yet, the spectra obtained from PMMA, PB, and PS are almost identical, even though the films are different thicknesses. Prior results showed a dependence on film thickness between samples that were several radius of gyration thick versus less than one radius of gyration thick. As noted in Sec. II, the radius of gyration provides a rough means of comparing different polymer samples rather than an absolute scaling. All the samples used for PS and PB were thicker than the radius of gyration for these polymers. Hence, we were not working in the regime where we would expect to observe the trend reported for PMMA. It was unclear from our previous study, where only two thicknesses were used, whether the spectra would continue to change as function of thickness. We hypothesized that the difference for the thinner films was caused by interaction with the substrate layer. Once films are thick enough that the substrate interactions no longer affect dynamics at the surface, the spectra should be identical. That we do not see a dependence of the probability of annihilating vibrational modes in the scattering process even though several different thicknesses were used in this study supports this hypothesis. Whether this is the same limit as the probability of annihilating modes in much thicker samples (>200 nm) or even the bulk limit is still unclear. We are currently investigating the onset of the thickness dependence on the surface vibrational modes to determine if this is uniform across different polymers and molecular weights.

To obtain information about the He-polymer potential energy surface, we fit the spectra for PMMA, PS, and PB to the semiclassical model described above. The unknown parameters for the polymer thin films are M, D, β, and Q_c. We have additionally included a scaling factor to normalize the predicted theoretical final flux to the experimental incident flux.[42] Of these parameters, the surface mass M and the Beeby correction D have the greatest influence on the multiphonon curve. We used several values for the surface mass, of which $M=15$ amu yielded the best fits. For PB and PS, such a value makes sense, as helium should interact with a hydrocarbon group, having a surface mass of 13 or 14 amu. As the model is not very sensitive to differences of 1 amu, we obtain good fits using $M=15$ amu. For PMMA and PS, SFG vibrational spectroscopy studies show that collisions are most likely to occur with surface masses of 15 and 13 amu, respectively.[37,38] The small surface mass for PMMA indicates that on the short time scale of the collision, helium is interacting primarily with the terminal methyl group, as seen previously for helium atom scattering from a fatty acid monolayer versus stiffer SAM systems.[33] We also use $D=7$ meV, as the Beeby correction should be similar as that for SAMs. We fit the spectra to determine β and Q_c. We used the model in two different ways, either fixing the scaling parameter for a set of temperature progressions, or letting it float in each fitting routine. We know that the flux will change for each temperature because the angular distribution shifts with increasing temperature.

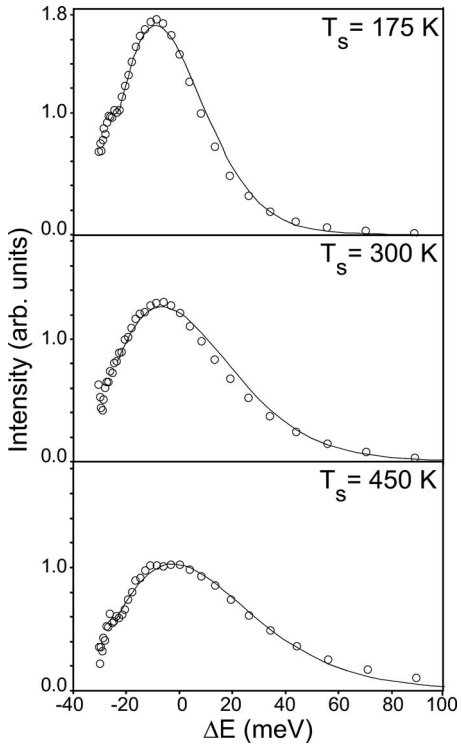

FIG. 9. The experimental scattering spectra (○) can be fit using a discrete semiclassical scattering model (—), as described in the text. The spectra shown are for polystyrene samples prepared on SiO_x/Si(100) with a thickness of 110.8 nm. The spectra were taken with a beam energy of 40 meV and an initial and final angles of 30.92°. The surface temperatures are listed for each plot. The values for β, Q_c, and the amplitude were allowed to vary for each surface temperature.

The model fits the lowest temperature curves well, considering the complexity of the model and the complexity of the system (Fig. 9). The values for β range from 1 to 3 Å^{-1} and remain constant across the wide range of surface temperatures and beam energies at which spectra were obtained. Since β represents the steepness of the repulsive part of the potential curve for the interaction between He and the surface in the absence of corrugation,[41] we have found that there is a large relative degree of interaction between He and the different polymer films. We have assumed only that the well depth of this interaction is roughly the same, but it appears that the shape of the repulsive part of the potential curve is also similar. Smaller values of β are indicative of softer surfaces. For example, single-phonon modes on close-packed metal surfaces tend to give β values of 2–3 Å^{-1}, whereas a rigid surface such as KCN has a β value of 5.5 Å^{-1}.[43]

We do not, however, see a pattern in the values obtained for Q_c. These values roughly fall between 2 and 8 Å^{-1}, and no trends are observed as the surface temperature is in-

creased. It is unclear if the fits we have performed are sensitive to Q_c values in this range. Q_c corresponds to the degree of surface roughness, as a rougher surface will scatter helium to larger values of parallel momentum.[43] Values in the determined range are indicative of higher surface corrugations.[40]

Simulations of thin hexadecane films (10–20 Å) on crystalline substrates demonstrate the degree of coarseness of these films.[44] While all films adsorb densely to the substrate, thinner films have a much larger free volume at the surface than thicker films due to the denser packing overall of the thicker films.[44] Yet, even the thicker films are atomically rough at the vacuum-organic interface. From simulations of decane films confined between two liquid interfaces, it is found that the roughness of the interface greatly increases between 300 and 400 K. Weaker interactions between chains lead to greater fluctuations at higher temperatures.[22] Simulations of monolayer films, such as amphiphiles on water also show an increase in interfacial coarsening as the temperature increases.[45] The increase in surface roughness with temperature is at least in part due to thermal fluctuations. We believe that the molecular coarsening is evident from the increase observed in the FWHM.

As seen from Eq. (2), the FWHM should have an inverse square-root dependence on the surface temperature. Thermal fluctuations cause an increase in surface roughness and are also responsible for the creation of capillary waves. The amplitude of the thermal roughness L is proportional to $(k_B T_s/\gamma)^{1/2}$, where γ is the surface tension.[46] In a study of rare gas scattering from liquids, the surface roughness was gauged by the growth of the thermal desorption peak. A "nearly" linear increase was observed and compared to the approximately linearly increasing values of $(T_s/\gamma)^{1/2}$. While rare gas scattering measures highly localized dynamics, whereas capillary waves occur over longer length scales, the coincidence is intriguing. King *et al.* hypothesize that there may be a correlation between dynamics on different length scales.[22] From this result, we conclude that to assign the functional form of the dependence of the FWHM on temperature, we may need to consider not only the multiphonon scattering process but also other surface structure at the polymer thin film interface.

It is interesting that our results show polymer surface dynamics to be remarkably similar, despite differences in substituent groups and glass transition temperatures. In rare gas scattering studies of squalane, glycerol, and Krytox 1625 (a perfluorinated polyether), King *et al.* demonstrate that these liquids can easily be identified by Ar scattering spectra.[22] They find that although Krytox 1625 has the highest compressibility and lowest surface tension of the liquids, it exhibits the lowest degree of energy transfer. They conclude that the scattering, specifically the impulsive energy transfer, is dependent on the local surface mass, where heavier functional groups absorb less energy during the short collision times.[47] Likewise, one of the first atomic scattering studies from SAMs showed that less energy is exchanged with molecules with CF_3 end groups than CH_3 end groups.[32] That our spectra are so similar suggests that the effective surface mass is the same for the three polymers. In Fig. 8, it is observed that the FWHM of the PMMA spectra is slightly smaller than for PS and PB, perhaps indicative of the slightly higher surface mass of 15 amu compared to 13 or 14 amu. To confirm this hypothesis, experiments with deuterated and undeuterated samples should be performed. It might also be instructive to use a higher energy, relatively nonpolarizable probe such as neon or argon in order to directly compare to the scattering literature on liquids. Such a study would allow us to determine whether the scattering spectra of the polymer thin films are more similar to the organic liquids or the atomic liquids, and hence, comment on the relative degree of energy transfer to confined polymers in comparison with liquids.

Probing with higher energy rare gas atoms rather than low-energy helium atoms allows us to access different but complimentary information about the characteristics of polymer thin films over the glass transition. Because low-energy helium atoms scatter from the electron density above the surface,[16] this technique is sensitive to mobility at the polymer-vacuum interface which may be, in turn, influenced by changes in the bulk of the polymer thin film. In contrast, a higher energy neutral probe will scatter from the surface of the polymer thin film and may penetrate the surface layer, as in the case of Xe scattering from a high density alkanethiol self-assembled monolayer.[48] Due to the increase in momentum, this rare gas probe is influenced by the overall elasticity of the surface. As a result, heavier rare gas probes are useful in obtaining information about both the surface and bulk of a material.

In an effort to look at higher energy scattering from the polymer thin films, we performed preliminary studies of neon atom scattering from PMMA. In the specular geometry, experiments were taken at angles of 24.42°, 32.42°, and 37.42° measured from the surface normal, a beam energy of 30 meV (17.0 $Å^{-1}$ with $\Delta K = 6.06$ $Å^{-1}$), and sample temperatures from 200 to 490 K. Angular distributions were taken using an incident angle of 32.42° and final angles from 24.42° to 37.42°. Neon does not have a tendency to thermalize with the surface, though the increase in momentum should broaden the inelastic feature observed with helium atom scattering and yield more information about the bulk of the polymer thin film. We observed the same qualitative results as observed from helium atom scattering from these studies. The low signal-to-noise ratio due to the long flight path and inherent low scattering signal obtained from polymers prevented us from investigating specific changes in line shape between helium and neon scattering.

Helium atom scattering provides different information than most prior studies of polymer thin film dynamics. While most studies in the literature measure the dynamics of long-range motion of polymer chains or segmental dynamics, helium atom scattering is most sensitive to surface vibrational dynamics of the topmost molecular layer. One of our goals in investigating polymer thin films has been to determine the behavior of the interface over the glass transition temperature T_g. Many previous studies have identified changes in chain segmental motion in the interfacial region as a function of temperature. Neutron scattering studies of thin films have shown that a difference in behavior of glassy systems arises around $1.2T_g$. Below this temperature, the increase in the

mean square displacement, $\langle u^2 \rangle$, is linear, while above $1.2T_g$, $\langle u^2 \rangle$ increases nonlinearly.[49] Changes in the mean square displacement should propagate to the surface region to which we are sensitive, and we will look for this change in more appropriate systems. In selecting future experiments, we want to further investigate whether the glass transition in the bulk of the thin film affects dynamics at the topmost interface.

VI. CONCLUSIONS

In summary, we have investigated the vibrational dynamics of polymer thin film interfaces with a precise and exclusively surface-sensitive probe, low-energy helium atom scattering. We have shown that the line shapes arising from helium atom scattering from PMMA, PB, and PS thin films are remarkably alike, having similar rates of intensity decay. Slight differences in the scattering are exhibited in the FWHM of these peaks, with PMMA having smaller values for the FWHM than PB and PS. The similarity between the spectra suggests that the helium beam interacts with groups of similar effective mass for the three polymers, in agreement with structural studies of the PMMA and PS interfaces. A discrete semiclassical model fits the line shape of the spectra well. This study has shown that polymers with different characteristics can have similar interfacial dynamics at the topmost interfacial layer.

ACKNOWLEDGMENTS

We thank K. Gibson for his insight and general help and J. Kreutz for preliminary work on sample preparation. This work was primarily supported by the Air Force Office of Scientific Research. We also received funding through the NSF-MRSEC at the University of Chicago, NSF-DMR-0213745. M.A.F. gratefully acknowledges support through a NSF Graduate Research Fellowship.

[1] K. Norrman, A. Ghanbari-Siahkali, and N. B. Larsen, Annu. Rep. Prog. Chem., Sect. C: Phys. Chem. **101**, 174 (2005); E. Pierstorff and D. Ho, J. Nanosci. Nanotechnol. **7**, 2949 (2007).
[2] M. Alcoutlabi and G. B. McKenna, J. Phys.: Condens. Matter **17**, R461 (2005); J. A. Forrest, Eur. Phys. J. E **8**, 261 (2002).
[3] G. Reiter, Europhys. Lett. **23**, 579 (1993); J. L. Keddie, R. A. L. Jones, and R. A. Cory, *ibid.* **27**, 59 (1994); J. L. Keddie, R. A. L. Jones, and R. A. Cory, Faraday Discuss. **98**, 219 (1994).
[4] J. A. Forrest, K. Dalnoki-Veress, and J. R. Dutcher, Phys. Rev. E **56**, 5705 (1997).
[5] Y. Grohens, L. Hamon, G. Reiter, A. Soldera, and Y. Holl, Eur. Phys. J. E **8**, 217 (2002); M. Beiner and H. Huth, Nat. Mater. **2**, 595 (2003).
[6] K. Dalnoki-Veress, J. A. Forrest, C. Murray, C. Gigault, and J. R. Dutcher, Phys. Rev. E **63**, 031801/1 (2001).
[7] L. Hartmann, W. Gorbatschow, J. Hauwede, and F. Kremer, Eur. Phys. J. E **8**, 145 (2002).
[8] D. B. Hall and J. M. Torkelson, Macromolecules **31**, 8817 (1998).
[9] R. D. Priestley, C. J. Ellison, L. J. Broadbelt, and J. M. Torkelson, Science **309**, 456 (2005).
[10] T. Kajiyama, K. Tanaka, and A. Takahara, Macromolecules **30**, 280 (1997).
[11] Q. F. Li, R. Hua, I. J. Cheah, and K. C. Chou, J. Phys. Chem. B **112**, 694 (2008).
[12] Z. Fakhraai and J. A. Forrest, Science **319**, 600 (2008); R. M. Papaléo, R. Leal, W. H. Carreira, L. G. Barbosa, I. Bello, and A. Bulla, Phys. Rev. B **74**, 094203/1 (2006).
[13] M. A. Freedman, A. W. Rosenbaum, and S. J. Sibener, Phys. Rev. B **75**, 113410/1 (2007).
[14] A. P. Graham, Surf. Sci. Rep. **49**, 115 (2003); *Helium Atom Scattering from Surfaces*, edited by E. Hulpke (Springer-Verlag, New York, 1992).
[15] G. Benedek and J. P. Toennies, Surf. Sci. **299–300**, 587 (1994); F. Hofmann and J. P. Toennies, Chem. Rev. (Washington, D.C.) **96**, 1307 (1996).
[16] J. P. Toennies, J. Phys.: Condens. Matter **5**, A25 (1993).
[17] L. W. Bruch, R. D. Diehl, and J. A. Venables, Rev. Mod. Phys. **79**, 1381 (2007).
[18] B. Poelsema, L. K. Verheij, and G. Comsa, Phys. Rev. Lett. **49**, 1731 (1982); L. Niu, D. J. Gaspar, and S. J. Sibener, Science **268**, 847 (1995).
[19] S. R. Cohen, R. Naaman, and J. Sagiv, Phys. Rev. Lett. **58**, 1208 (1987); N. Camillone, C. E. D. Chidsey, G.-y. Liu, T. M. Putvinski, and G. Scoles, J. Chem. Phys. **94**, 8493 (1991); S. B. Darling, A. M. Rosenbaum, and S. J. Sibener, Surf. Sci. **478**, L313 (2001); A. W. Rosenbaum, M. A. Freedman, S. B. Darling, I. Popova, and S. J. Sibener, J. Chem. Phys. **120**, 3880 (2004); S. Vollmer, P. Fouquet, G. Witte, C. Boas, M. Kunat, U. Burghaus, and C. Wöll, Surf. Sci. **462**, 135 (2000).
[20] B. F. Mason and B. R. Williams, Surf. Sci. **130**, 295 (1983); **130**, L329 (1983); **139**, 173 (1984).
[21] A. P. Graham, J. Chem. Phys. **115**, 524 (2001).
[22] M. E. King, M. E. Saecker, and G. M. Nathanson, J. Chem. Phys. **101**, 2539 (1994).
[23] V. Vogel and C. Wöll, Thin Solid Films **159**, 429 (1988).
[24] K. D. Gibson, N. Isa, and S. J. Sibener, J. Chem. Phys. **119**, 13083 (2003).
[25] *Polymer Handbook*, edited by J. Brandrup, E. H. Immergut, and E. A. Grulke (Wiley, Hoboken, NJ, 1999).
[26] L. Niu, D. D. Koleske, D. J. Gaspar, and S. J. Sibener, J. Chem. Phys. **102**, 9077 (1995); B. Gans, P. A. Knipp, D. D. Koleske, and S. J. Sibener, Surf. Sci. **264**, 81 (1992).
[27] K. Sköld, Nucl. Instrum. Methods **63**, 114 (1968); D. D. Koleske and S. J. Sibener, Rev. Sci. Instrum. **63**, 3852 (1992).
[28] G. Comsa, R. David, and B. J. Schumacher, Rev. Sci. Instrum. **52**, 789 (1981).
[29] M. R. Houston and R. Maboudian, J. Appl. Phys. **78**, 3801 (1995).
[30] T. Kashiwagi, A. Inaba, J. E. Brown, K. Hatada, T. Kitayama, and E. Masuda, Macromolecules **19**, 2160 (1986).
[31] D. W. Brazier and N. V. Schwartz, J. Appl. Polym. Sci. **22**, 113 (1978); B. Schneider, D. Doskočilová, J. Štokr, and M. Svoboda, Polymer **34**, 432 (1993).
[32] S. R. Cohen, R. Naaman, and J. Sagiv, Phys. Rev. Lett. **58**, 1208 (1987).
[33] J. R. Manson and J. G. Skofronick, Phys. Rev. B **47**, 12890 (1993).
[34] C.-f. Yu, K. B. Whaley, C. S. Hogg, and S. J. Sibener, J. Chem. Phys. **83**, 4217 (1985).
[35] J. L. Beeby, J. Phys. C **4**, L359 (1971).
[36] N. Camillone III, C. E. D. Chidsey, G.-y. Liu, T. M. Putvinski, and G. Scoles, J. Chem. Phys. **94**, 8493 (1991).
[37] J. Wang, C. Chen, S. M. Buck, and Z. Chen, J. Phys. Chem. B **105**, 12118 (2001).
[38] K. S. Gautam, A. D. Schwab, A. Dhinojwala, D. Zhang, S. M. Dougal, and M. S. Yeganeh, Phys. Rev. Lett. **85**, 3854 (2000); K. A. Briggman, J. C. Stephenson, W. E. Wallace, and L. J. Richter, J. Phys. Chem. B **105**, 2785 (2001).
[39] J. R. Manson, V. Celli, and D. Himes, Phys. Rev. B **49**, 2782 (1994).
[40] F. Hofmann, J. P. Toennies, and J. R. Manson, J. Chem. Phys. **106**, 1234 (1997).
[41] M. Li, J. R. Manson, and A. P. Graham, Phys. Rev. B **65**, 195404/1 (2002).
[42] D. J. Gaspar, A. T. Hanbicki, and S. J. Sibener, J. Chem. Phys. **109**, 6947 (1998).
[43] S. M. Weera, J. R. Manson, J. Baker, E. S. Gillman, J. J. Hernández, G. G. Bishop, S. A. Safron, and J. G. Skofronick, Phys. Rev. B **52**, 14185 (1995).
[44] T. K. Xia, J. Ouyang, M. W. Ribarsky, and U. Landman, Phys. Rev. Lett. **69**, 1967 (1992).
[45] J. Harris and S. A. Rice, J. Chem. Phys. **89**, 5898 (1988).
[46] D. G. A. L. Aarts, Soft Matter **3**, 19 (2007).
[47] M. E. Saecker and G. M. Nathanson, J. Chem. Phys. **100**, 3999 (1994).
[48] K. D. Gibson, N. Isa, and S. J. Sibener, J. Phys. Chem. A **110**, 1469 (2006).
[49] C. L. Soles, J. F. Douglas, W.-I. Wu, and R. M. Dimeo, Macromolecules **36**, 373 (2003).